Autoparametric Resonance in Mechanical Systems

Aleš Tondl
Thijs Ruijgrok
Ferdinand Verhulst
Radoslav Nabergoj

CAMBRIDGE
UNIVERSITY PRESS

PUBLISHED BY THE PRESS SYNDICATE OF THE UNIVERSITY OF CAMBRIDGE
The Pitt Building, Trumpington Street, Cambridge, United Kingdom

CAMBRIDGE UNIVERSITY PRESS
The Edinburgh Building, Cambridge CB2 2RU, UK http://www.cup.cam.ac.uk
40 West 20th Street, New York, NY 10011-4211, USA http://www.cup.org
10 Stamford Road, Oakleigh, Melbourne 3166, Australia
Ruiz de Alarcón 13, 28014 Madrid, Spain

First published 2000

Printed in the United States of America

Typeface Times Roman 11/14 pt. and Futura *System* LaTeX 2_ε [TB]

A catalog record for this book is available from the British Library.

Library of Congress Cataloging in Publication Data

Autoparametric resonance in mechanical systems / Aleš Tondl . . . [et al.].
p. cm.
Includes bibliographical references (p.).
ISBN 0-521-65079-8 (hardbound)
1. Parametric vibration. 2. Damping (Mechanics) 3. Nonlinear theories. 4. Differentiable dynamical systems. I. Tondl, Aleš.
TA355.A88 2000
620.3 – dc21 99-38309
CIP

ISBN 0 521 65079 8 hardback

Contents

Chapter 2

Basic Properties

2.1 Introductory Examples

The examples presented in this chapter are artificial in the sense that they were not proposed to model real-life problems, but to analyse and demonstrate the basic properties of autoparametric systems with examples as simple as possible. Note that for these systems we need at least 2 degrees of freedom and a nonlinear, resonant interaction. The examples can be viewed as realistic when we consider them as modeling single-mass systems with 2 degrees of freedom. We return to this point of view in some elementary examples discussed in Chapter 3.

We consider three examples, each consisting of two subsystems that have 1 degree of freedom. Each example contains a different kind of primary system, characterised subsequently by external excitation, parametric excitation, and self-excitation. The first system is characterised by an externally excited primary system. The governing equations, transformed into dimensionless form, are

$$x'' + \kappa_1 x' + x + \gamma_1 y^2 = a\eta^2 \cos \eta\tau,$$
$$y'' + \kappa_2 y' + q^2 y + \gamma_2 xy = 0, \qquad (2.1.1)$$

where $\kappa_1 > 0$ and $\kappa_2 > 0$ are the damping coefficients, γ_1 and γ_2 are the nonlinear coupling coefficients, $q = \omega_2/\omega_1$ is the tuning coefficient that expresses the ratio of natural frequencies of the undamped linearised secondary system and the primary system, $a\eta^2$ expresses the amplitude of the external excitation, and $\eta = \omega/\omega_1$ is the forcing frequency. Here, ω is the dimensional frequency of the excitation and ω_1 and ω_2 are the natural frequencies of the primary system and the secondary system, respectively.

The second system is an example of a parametrically excited primary system that is governed by the following equations of motion:

$$\begin{aligned} x'' + \kappa_1 x' + (1 + a\cos 2\eta\tau)x + \gamma_1(x^2 + y^2)x = 0, \\ y'' + \kappa_2 y' + q^2 y + \gamma_2 xy = 0, \end{aligned} \qquad (2.1.2)$$

where κ_1, κ_2, γ_1, γ_2, and q are coefficients similar to those for the first system, η is the excitation frequency, and a is the coefficient of the parametric-excitation term.

The third system contains a self-excited primary system. This system is governed by the following equations of motion:

$$\begin{aligned} x'' - (\beta - \delta x'^2)x' + x + \gamma_1 y^2 = 0, \\ y'' + \kappa y' + q^2 y + \gamma_2 xy = 0, \end{aligned} \qquad (2.1.3)$$

where κ, γ_1, γ_2, and q have meanings similar to those of the preceding cases and $\beta > 0$ and $\delta > 0$ are the coefficients of the terms representing the self-excitation of Rayleigh type.

In the first and the third examples we have chosen the term $\gamma_1 y^2$ as the nonlinear coupling term in the equation for the primary system. This choice was made because $\gamma_1 y^2$ is the lowest-order term that produces a resonant interaction when $\omega_1 : \omega_2 = 2 : 1$. It is precisely this resonance that is studied.

In the second example, however, restricting the coupling term to $\gamma_1 y^2$ would not lead to a bounded semitrivial solution. We have therefore chosen $\gamma_1(x^2 + y^2)x$ as the coupling term in this example. Such a term might arise, for instance, when the underlying system is symmetric under $x \to -x$. This situation occurs in the single-mass system studied in Chapter 3.

The coupling term $\gamma_2 xy$ in the secondary system is the same for the three alternatives, again for the sake of simplicity. In each system we obtain the semitrivial solution by putting $y = 0$, $y' = 0$. The choice of the coupling terms affects the type of autoparametric resonance that occurs in the system. We discuss this problem in Section 2.5.

2.2 A System with External Excitation

2.2.1 The Semitrivial Solution and Its Stability

To find the semitrivial solution of Eq. (2.1.1) we put

$$x(\tau) = R\cos(\eta\tau + \psi_1), \quad y(\tau) = 0. \tag{2.2.1}$$

This yields the solution for R:

$$R = R_0 = \frac{a\eta^2}{\Delta^{1/2}}, \quad \Delta = (1-\eta^2)^2 + \kappa_1^2\eta^2. \tag{2.2.2}$$

Note that when $\kappa_1 = \mathcal{O}(\varepsilon)$ and $\eta = 1 + \mathcal{O}(\varepsilon)$, the amplitude of the semitrivial solution is $R_0 = \mathcal{O}(a/\varepsilon)$. This situation is related to the main resonance for the primary system, and it will be one of the cases under consideration.

The stability investigation of the semitrivial solution will show the intervals of the excitation frequency where this semitrivial solution is unstable and a nontrivial solution will arise. Inserting the expressions

$$x = R_0\cos(\eta\tau + \psi_1) + u, \quad y = 0 + v,$$

into Eqs. (2.1.1) then yields, in linear approximation,

$$\begin{aligned} u'' + \kappa_1 u' + u &= 0, \\ v'' + \kappa_2 v' + [q^2 + \gamma_2 R_0\cos(\eta\tau + \psi_1)]v &= 0. \end{aligned} \tag{2.2.3}$$

The solution $u = 0$ of the first equation of Eqs. (2.2.3) is asymptotically stable. Thus the second equation of Eqs. (2.2.3) fully determines the stability of the semitrivial solution. This equation is of Mathieu type, and its main instability domain is found for values of q near $\frac{1}{2}\eta$. The Mathieu equation is discussed in fuller detail in Chapter 9.

We assume κ_2 and γ_2 to be small, and we write

$$\kappa_2 = \varepsilon\hat{\kappa}_2, \quad \gamma_2 = \varepsilon\hat{\gamma}_2, \quad q^2 = \tfrac{1}{4}\eta^2 + \varepsilon\sigma_2.$$

Putting $v_1 = v$, $v_2 = v'$ and translating the time variable so that $\psi_1 = 0$

gives the equations

$$\begin{aligned} v_1' &= v_2, \\ v_2' &= -\tfrac{1}{4}\eta^2 v_1 - \varepsilon(\kappa_2 v_2 + \sigma_2 v_1 + \gamma_2 R_0 \cos\eta\tau\, v_1), \end{aligned} \tag{2.2.4}$$

where it is assumed that $R_0 = \mathcal{O}(1)$ as $\varepsilon \to 0$ and the hats have been dropped. We subsequently leave out the limit $\varepsilon \to 0$, as it is assumed that ε is always a small parameter.

As in Section 9.5, the boundary of the main instability domain can be found by use of the averaging method. We find to first order in ε that

$$\sigma_2^2 + \tfrac{1}{4}\kappa_2^2\eta^2 - \tfrac{1}{4}\gamma_2^2 R_0^2 = 0. \tag{2.2.5}$$

Two different approaches on how to use condition (2.2.5) can be applied. The first one of these can be called the excitation-oriented approach and the second the response-oriented approach. We describe these two methods in Subsections 2.2.2 and 2.2.3, respectively.

2.2.2 Excitation-Oriented Approach

In the first approach, the expressions for R_0 from Eqs. (2.2.2) are inserted into Eq. (2.2.5). This yields the critical value a_c for the excitation amplitude:

$$a_c = \frac{\Delta^{1/2}}{\gamma_2\eta^2}\left(\sigma_2^2 + \kappa_2^2\eta^2\right)^{1/2}. \tag{2.2.6}$$

For values of a above this critical value the semitrivial solution is unstable. In particular, from Eq. (2.2.6) it follows that when $\eta = 1 + \mathcal{O}(\varepsilon)$ then $\Delta^{1/2} = \mathcal{O}(\varepsilon)$ and so also $a_c = \mathcal{O}(\varepsilon)$.

As an example, in Figure 2.1 the instability threshhold $\gamma_2 a_c$ of the semitrivial solution is shown. Note that we have multiplied the amplitude of excitation a by the coefficient of nonlinearity γ_2. Also, to obtain a more convenient representation, the direction of the $\gamma_2 a$ axis has been changed so that minima appear as maxima and the instability domain now lies below the surface. The system parameters κ_1 and κ_2 are given in the diagrams directly. Moreover, in the (η, q) plane the lines $\eta = 1$ and $\eta = 2q$ are marked. The figure shows that close to $\eta = 1$ and $\eta = 2q$ the instability threshhold exhibits local minima.

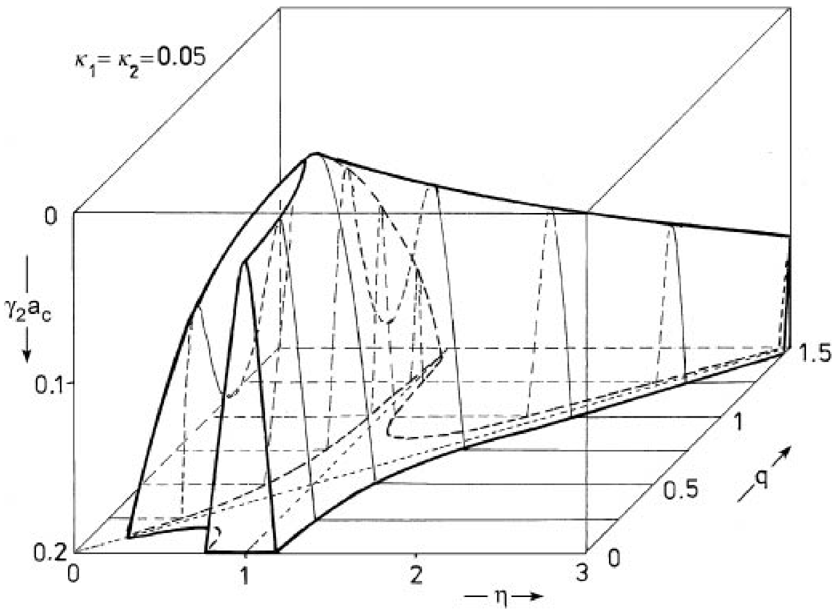

Figure 2.1: Axonometric representation of the instability threshhold $\gamma_2 a_c$ of the semitrivial solution. The instability region is below the surface. The values of the parameters are $\kappa_1 = \kappa_2 = 0.05$.

2.2.3 Response-Oriented Approach

In this approach, we use the amplitude of the response rather than the amplitude of the excitation to characterise the stability of the semitrivial solution. In many applications this is the preferred method. The amplitude of the response is R_0, so from Eq. (2.2.5) it follows that the critical value of R_0 (i.e., where the semitrivial solution loses stability) is given by

$$R_0 = R_c(\eta) = \frac{1}{\gamma_2}\left(\sigma_2^2 + \kappa_2^2\eta^2\right)^{1/2}. \tag{2.2.7}$$

Plotting $R_c(\eta)$ together with the amplitude $R_0(\eta)$ of the semitrivial solution in an amplitude-frequency diagram gives the values of the frequency η for which the semitrivial solution is unstable.

This is demonstrated in Figure 2.2 by an example with the following parameter values: $\kappa_1 = 0.10$, $\kappa_2 = 0.05$, $\gamma_2 = 0.10$, and $q = 0.75$. The

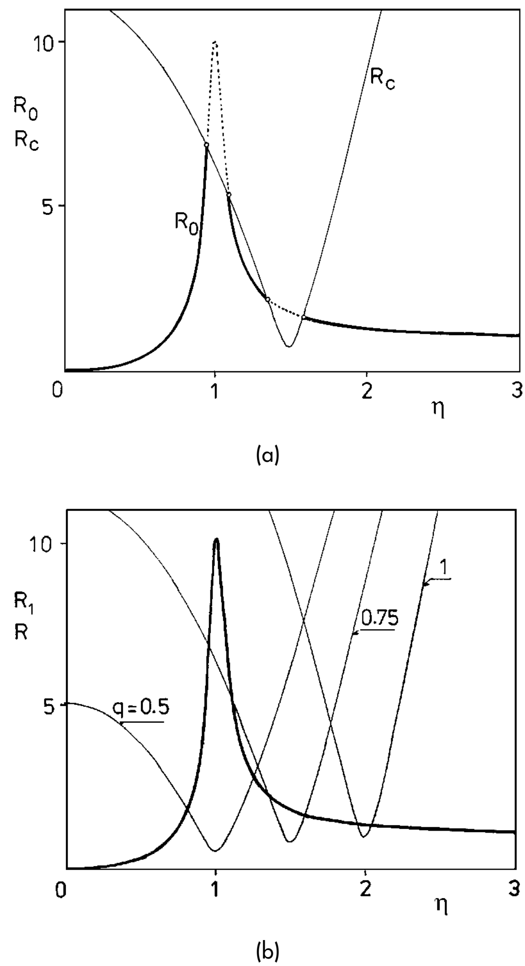

Figure 2.2: Vibration amplitude curve R_0 corresponding to the semitrivial solution (stable solution, heavy solid curves; unstable solution, dotted curves) and the stability boundary curve R_c (light solid curves) as functions of the excitation frequency η. The following values have been used: $\kappa_1 = 0.10$, $\kappa_2 = 0.05$, $\gamma_2 = 0.10$, $q = 0.75$.

figure shows the frequency response curve $R_0(\eta)$ as well as $R_c(\eta)$, the latter marked by a solid light curve. Parts of the curve to which unstable solutions correspond are indicated by dotted curves. As we can see, there exist unstable parts in the response, and these are located near $\eta = 1$ and $\eta = 2q$, in accordance with the preceding analysis.

2.2.4 Nontrivial Solution

We now look for a nontrivial periodic solution in the case in which $q \approx \frac{1}{2}\eta$. As was noted in Subsection 2.2.3, we must then take $a = \mathcal{O}(\varepsilon)$. Rescaling Eqs. (2.1.1) through

$$a = \varepsilon\hat{a}, \quad \kappa_1 = \varepsilon\hat{\kappa}_1, \quad \gamma_1 = \varepsilon\hat{\gamma}_1,$$
$$\eta^2 = 1 - \varepsilon\sigma_1, \quad q^2 = \tfrac{1}{4}\eta^2 + \varepsilon\sigma_2,$$

gives the following equations (with the hats dropped):

$$\begin{aligned} x'' + \eta^2 x &= -\varepsilon(\kappa_1 x' + \sigma_1 x + \gamma_1 y^2 - a\eta^2 \cos \eta\tau), \\ y'' + \tfrac{1}{4}\eta^2 y &= -\varepsilon(\kappa_2 y' + \sigma_2 y + \gamma_2 xy). \end{aligned} \tag{2.2.8}$$

For $\varepsilon = 0$, the solutions to Eqs. (2.2.8) can be written as

$$x = R_1 \cos(\eta\tau + \psi_1), \quad y = R_2 \cos\left(\tfrac{1}{2}\eta\tau + \psi_2\right).$$

A $4\pi/\eta$-periodic solution can be found with the Poincaré–Lindstedt method (see Chapter 9). This method leads to the following system of conditions, up to $\mathcal{O}(\varepsilon)$:

$$\begin{aligned} \sigma_1 R_1 + \tfrac{1}{2}\gamma_1 R_2^2 \cos(\psi_1 - 2\psi_2) - a \cos\psi_1 &= 0, \\ \kappa_1 R_1 - \tfrac{1}{2}\gamma_1 R_2^2 \sin(\psi_1 - 2\psi_2) + a \sin\psi_1 &= 0, \\ \sigma_2 R_2 + \tfrac{1}{2}\gamma_2 R_1 R_2 \cos(\psi_1 - 2\psi_2) &= 0, \\ -\kappa_2 R_2 - \gamma_2 R_1 R_2 \sin(\psi_1 - 2\psi_2) &= 0. \end{aligned} \tag{2.2.9}$$

Note that $\eta = 1 + \mathcal{O}(\varepsilon)$; therefore we have replaced expressions such as $a\eta^2$ and $\kappa_1\eta$ with a and κ_1.

The vibration amplitude of the x coordinate follows from the last two equations of system (2.2.9), and the result is

$$R_1 = \frac{2}{\gamma_2}\left(\sigma_2^2 + \tfrac{1}{4}\kappa_2^2\right)^{1/2}. \tag{2.2.10}$$

From the first two equations of system (2.2.9) the following quadratic equation for the amplitude of the y coordinate is obtained:

$$z^2 + Bz + A = 0, \quad z = \tfrac{1}{2}\gamma_1\gamma_2 R_2^2, \tag{2.2.11}$$

with

$$A = 4(\sigma_1^2 + \kappa_1^2)(\sigma_2^2 + \kappa_2^2) - \gamma_2^2 a^2,$$
$$B = 4(\kappa_1\kappa_2 - \sigma_1\sigma_2). \tag{2.2.12}$$

Let $D = B^2 - 4A = 16[\frac{1}{4}\gamma_2^2 a^2 - (\sigma_1\kappa_2 + \sigma_2\kappa_1)^2]$; then Eq. (2.2.11) has no solutions if $A > 0$ and $D < 0$, two solutions if $A > 0$ and $D > 0$, and one solution if $A < 0$, irrespective of the value of D. Note that the condition $A < 0$ is equivalent to

$$a > \frac{2}{\gamma_2}(\sigma_1^2 + \kappa_1^2)^{1/2}(\sigma_2^2 + \kappa_2^2)^{1/2} = a_c. \tag{2.2.13}$$

In other words, $A < 0$ is equivalent to the condition that the semitrivial solution is unstable. So in this case system (2.1.1) has an unstable semitrivial solution and a stable periodic solution. If $A > 0$ the situation is more complicated.

In this system we see the so-called saturation phenomenon occurring. Assume that all the parameters except a are constant and such that $B > 0$. Letting a increase from 0 to a_c, we see that the stable response of the system will be the semitrivial solution. From Eqs. (2.2.2) it follows that the amplitude of this solution, which is given by

$$R_0 = \frac{a}{(\sigma_1^2 + \kappa_1^2)^{1/2}},$$

grows linearily with a. At $a = a_c$ the semitrivial solution loses stability in a supercritical period-doubling bifurcation. The amplitude of the (semitrivial) response is then

$$R_0 = \frac{a_c}{(\sigma_1^2 + \kappa_1^2)^{1/2}} = \frac{2}{\gamma_2}(\sigma_1^2 + \kappa_1^2)^{1/2}.$$

When $a > a_c$, it follows from Eq. (2.2.10) that the x component of the response remains constant when a is increased. The y component, which can be calculated by the solution of Eq. (2.2.11), grows with increasing a. Thus, when the excitation amplitude is increased, the portion of the energy supplied by the external source to the primary system remains constant and the whole increment of energy flows to the excited subsystem.

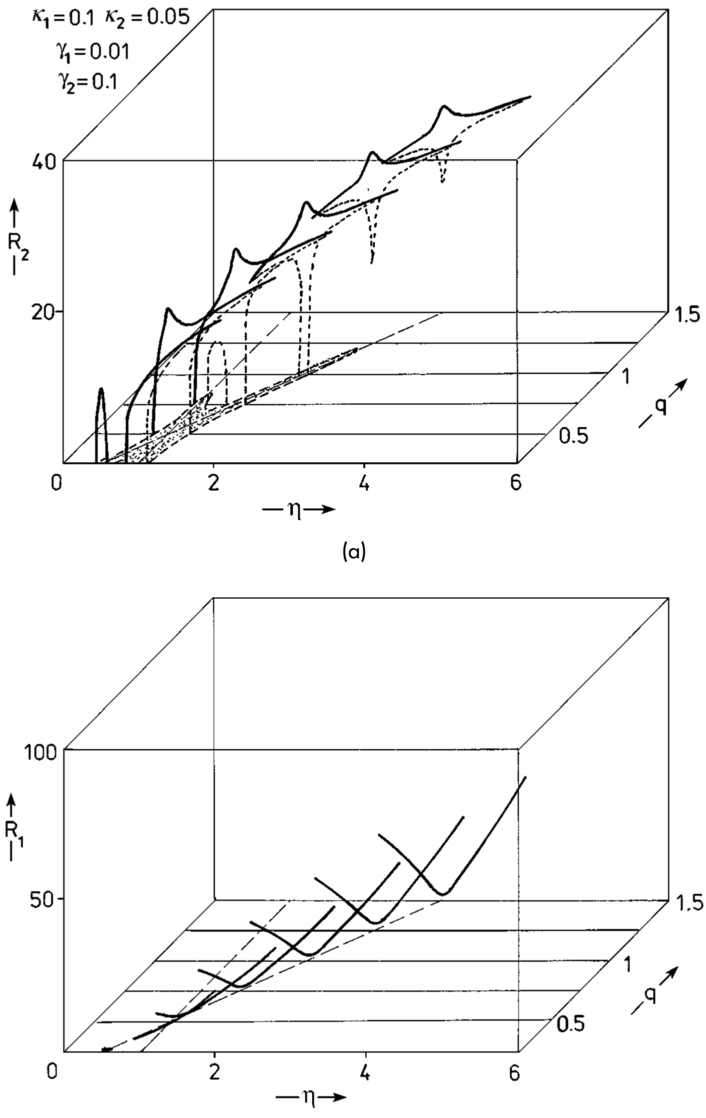

Figure 2.3: Vibration amplitude curves R_1 and R_2 corresponding to the nontrivial solution as functions of the excitation frequency η and tuning ratio q. Stable solutions are marked by solid curves and unstable solutions by dotted curves. The following values have been used: $\kappa_1 = 0.1$, $\kappa_2 = 0.05$, $\gamma_1 = 0.01$, $\gamma_2 = 0.10$.

In Figures 2.3 we have plotted the values of R_1 and R_2 as functions of q and η for specific values of the parameters κ_1, κ_2, γ_1, and γ_2. These curves are arranged in axonometric view, and the values are marked directly in the diagrams. Parts of the curves corresponding to stable solutions are marked by heavy solid curves. The unstable solutions are marked by dashed lines. In the (η, q) plane bias, the scale lines for certain constant values of q are marked by light solid straight lines interrupted in those intervals of η where, for certain values of the excitation frequency, only one solution of R_2 for the nontrivial solution exists. This area in the (η, q) plane is dotted and its boundary is marked by a dashed curve. These diagrams show that the domain of existence of the stable nontrivial solution is broader than that of the semitrivial solution instability. It follows that there exist frequency intervals where two locally stable periodic solutions exist: both the semitrivial solution and a nontrivial solution (autoparametric resonance), and consequently two domains of attraction as well.

To illustrate the transient behaviour of the system when the excitation frequency η is slowly increased and subsequently decreased, the values of $R_1(\eta)$ and $R_2(\eta)$ are shown in Figure 2.4 for $q = 0.25$ and 0.75 and for the following parameter values: $\kappa_1 = 0.10$, $\kappa_2 = 0.05$, $\gamma_1 = 0.01$, and $\gamma_2 = 0.10$. It can be seen that there exists one interval of η where two locally stable solutions exist. At the boundary of this interval the character of the solution changes by a jump.

2.3 A Parametrically Excited System

2.3.1 The Semitrivial Solution and Its Stability

After the equations of motion are rescaled and the hats are dropped, the semitrivial solution of Eqs. (2.1.2) is given by $y = 0$ and x a solution of

$$x'' + \varepsilon\kappa_1 x' + (\eta^2 + \varepsilon a \cos 2\eta\tau)x + \varepsilon\sigma_1 x + \varepsilon\gamma_1 x^3 = 0. \quad (2.3.1)$$

Assuming that $x = R_0 \cos(\eta\tau + \psi_0)$, we can find equations for R_0 and ψ_0. After averaging over τ and a time scaling, these become

$$R_0' = -\kappa_1 \eta R_0 + \tfrac{1}{2} a R_0 \sin 2\psi_1,$$

$$\psi_0' = \sigma_1 + \tfrac{1}{2} a \cos 2\psi_1 + \tfrac{3}{4}\gamma_1 R_0^2. \quad (2.3.2)$$

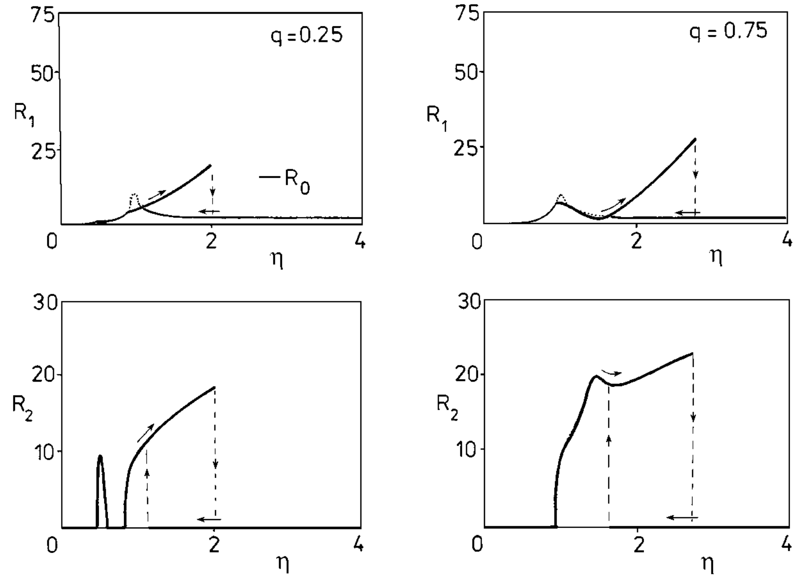

Figure 2.4: Vibration amplitude curves $R_1 = R_1(\eta)$ and $R_2 = R_2(\eta)$ corresponding to the non-trivial solution when the excitation frequency η is increased and subsequently decreased. The arrows mark the sense of changes and jumps. The following values have been used: $\kappa_1 = 0.10$, $\kappa_2 = 0.05$, $\gamma_1 = 0.01$, $\gamma_2 = 0.10$, $q = 0.25$ and 0.75.

Equilibrium solutions of Eqs. (2.3.2) correspond to $2\pi/\eta$-periodic solutions. We find that the amplitude of these periodic solutions is given by

$$R_0^2 = \tfrac{4}{3}\frac{1}{\gamma_1}\left[-\sigma_1 \pm \left(\tfrac{1}{4}a^2 - \kappa_1^2\eta^2\right)^{1/2}\right]. \qquad (2.3.3)$$

From the averaged equations it follows that the plus sign corresponds to a stable solution of Eq. (2.3.1) and the minus sign to an unstable solution. The stability of the semitrivial solution is determined by

$$y'' + \varepsilon\kappa_2 y' + \tfrac{1}{4}\eta^2 y + \varepsilon\sigma_2 y + \varepsilon\gamma_2 r_0 \cos\eta\tau y = 0, \qquad (2.3.4)$$

where r_0 is the solution of Eq. (2.3.3) corresponding to the plus sign. The boundary of the main instability domain is, to first order in ε, given by

$$\tfrac{1}{4}\gamma_2^2 r_0^2 = \sigma_2^2 + \tfrac{1}{4}\kappa_2^2\eta^2. \qquad (2.3.5)$$

Note that this result is very similar to Eq. (2.2.5) in the preceding example.

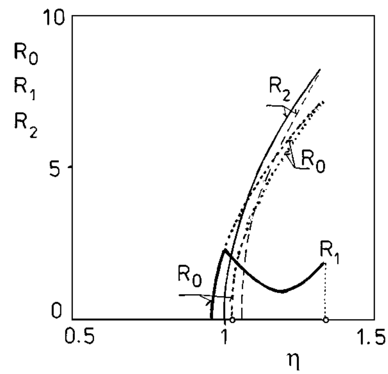

Figure 2.5: Vibration amplitude curves R_0, R_1, and R_2 corresponding to the semitrivial and the nontrivial solution as functions of the excitation frequency η. Stable solutions are marked by solid curves and unstable solutions by dashed and dotted curves. The following values have been used: $\kappa_1 = \kappa_2 = 0.075$, $\gamma_1 = 0.02$, $\gamma_2 = 0.10$, $\varepsilon = 0.20$, $q = 0.60$.

2.3.2 Nontrivial Solution

Nontrivial solutions can be found as in Subsection 2.3.1 by the introduction of

$$x = R_1 \cos(\eta\tau + \psi_1), \quad y = R_2 \cos\left(\tfrac{1}{2}\eta\tau + \psi_2\right).$$

Applying the Poincaré–Lindstedt method then yields the following set of conditions:

$$\begin{aligned}
-\kappa_1 \eta R_1 + \tfrac{1}{2} a R_1 \sin 2\psi_1 &= 0,\\
\sigma_1 + \tfrac{1}{2} a \cos 2\psi_1 + \tfrac{3}{4}\gamma_1 R_1^2 + \tfrac{1}{2}\gamma_1 R_2^2 &= 0,\\
-\tfrac{1}{2}\kappa_2 \eta R_2 - \tfrac{1}{2}\gamma_2 R_1 R_2 \sin(\psi_1 - 2\psi_2) &= 0,\\
\sigma_2 + \tfrac{1}{2}\gamma_2 R_1 \cos(\psi_1 - 2\psi_2) &= 0.
\end{aligned} \tag{2.3.6}$$

This yields

$$\begin{aligned}
\tfrac{1}{4}\gamma_2^2 R_1^2 &= \sigma_2^2 + \tfrac{1}{4}\kappa_2^2 \eta^2,\\
\tfrac{1}{2}\gamma_1 R_2^2 &= -\tfrac{3}{4}\gamma_1 R_1^2 - \sigma_1 \pm \left(\tfrac{1}{4}a^2 - \kappa_1^2 \eta^2\right)^{1/2}.
\end{aligned} \tag{2.3.7}$$

As in the preceding example, we have a saturation phenomenon. The following parameter values are taken for explicit examples: $\kappa_1 = \kappa_2 = 0.075$, $\gamma_1 = 0.02$, $\gamma_2 = 0.10$, and $\varepsilon = 0.20$. In Figure 2.5, we

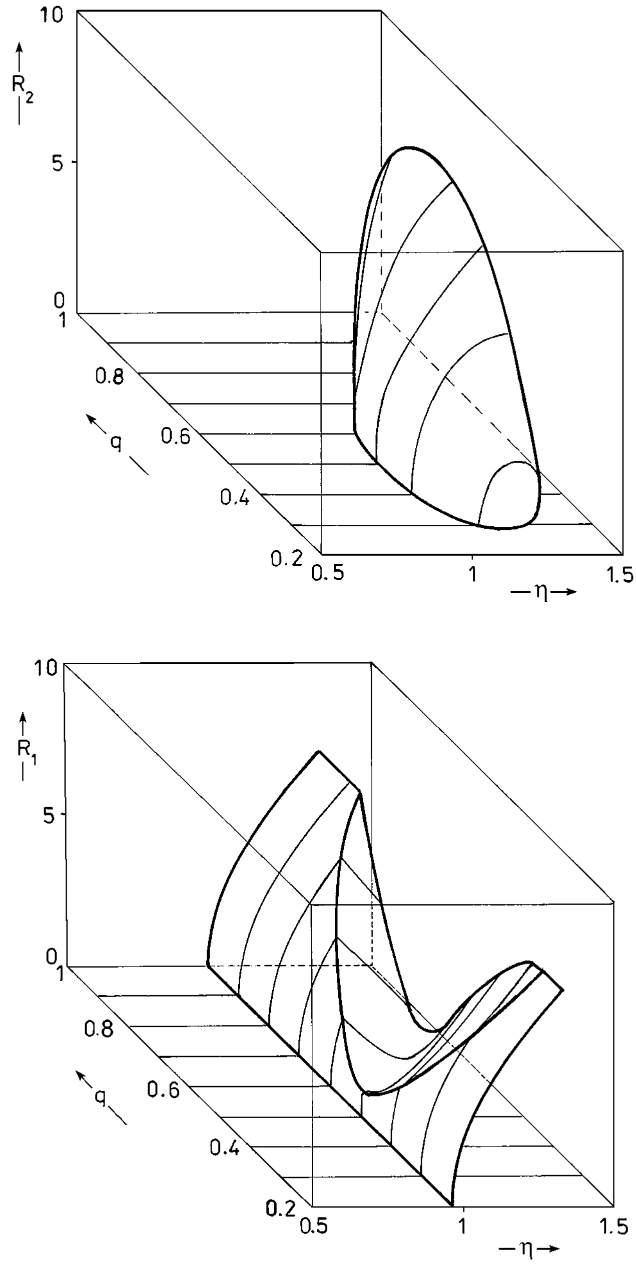

Figure 2.6: Axonometric representation of the stable vibration amplitudes R_1 and R_2 corresponding to the nontrivial solution as functions of the excitation frequency η and tuning ratio q. The following values have been used: $\kappa_1 = \kappa_2 = 0.075$, $\gamma_1 = 0.02$, $\gamma_2 = 0.10$, $\varepsilon = 0.20$.

show the amplitudes R_0, R_1, R_2 as functions of η for the case $q = 0.60$; the solid curves represent stable solutions and the dashed or dotted ones represent unstable solutions. Again there is an interval of η where both semitrivial and nontrivial solutions exist, their realisation depending on initial conditions. This instability interval lies between the points on the η axis marked by circles.

To illustrate the influence of the tuning coefficient q, Figure 2.6 shows in axonometric view the amplitudes R_1 (both semitrivial and nontrivial solutions) and R_2 as functions of η and q (only stable solutions). We can see that there exists only one interval of q where autoparametric resonance is initiated, i.e., in the neighbourhood of $q = \frac{1}{2}\eta$. The domain of autoparametric resonance occurrence is relatively narrower compared with the system that has an externally excited primary system.

2.4 A Self-Excited System

2.4.1 The Semitrivial Solution and Its Stability

In contrast with the preceding two examples, system (2.1.3) is autonomous, so the periodic solutions will not have a definite phase associated with them. After the equations of motion are rescaled and the carets are dropped, the semitrivial solution of system (2.1.3) is given by $y = 0$, $y' = 0$, and x a solution of

$$x'' - \varepsilon(\beta - \delta x'^2)x' + x = 0. \tag{2.4.1}$$

Writing $x = R_0 \cos(\tau + \psi_0)$ and averaging over τ yields the equations

$$\begin{aligned} R_0' &= \tfrac{1}{2}\varepsilon\left(\beta R_0 - \tfrac{3}{4}\delta R_0^3\right), \\ \psi_0' &= 0. \end{aligned} \tag{2.4.2}$$

From the averaged equations, we find a stable periodic orbit with amplitude

$$R_0 = \left(\tfrac{4}{3}\frac{\beta}{\delta}\right)^{1/2}. \tag{2.4.3}$$

Using the same method as in the two preceding examples, we find that